Turkish Journal of Electrical Engineering & Computer Sciences

http://journals.tubitak.gov.tr/elektrik/

Research Article

Turk J Elec Eng & Comp Sci
(2018) 26: 2753 – 2767

doi:10.3906/elk-1712-153

A new technique for optimum excitation of switched reluctance motor drives over a wide speed range

Mahmoud HAMOUDA[1,2,*], **László SZÁMEL**[2]

[1]Department of Electrical Engineering, Faculty of Engineering, Mansoura University, Mansoura, Egypt
[2]Department of Electric Power Engineering, Faculty of Electrical Engineering and Informatics, Budapest University of Technology and Economics, Budapest, Hungary

Received: 11.12.2017 • **Accepted/Published Online:** 15.04.2018 • **Final Version:** 28.09.2018

Abstract: Optimum performance of switched reluctance motors (SRMs) over a wide range of speed control is an essential approach for many industrial applications. However, the doubly salient structure and deep magnetic saturation make magnetization characteristics of SRMs a highly nonlinear function of rotor position and current magnitude. This, in turn, makes the control of SRM drives a challenging task. As the control of SRMs depends on the inductance profile, it requires an adaptive control technique for optimum operation over a wide range of operating speeds. This paper presents an adaptive control technique for optimum excitation of SRM drives. The proposed control technique accurately considers the effect of back-emf voltage for high- and even low-speed operation. It determines the most efficient switch-on angle as a function of motor speed and current magnitude. Moreover, the optimum switch-off angle is defined to enhance motor output torque/power without negative torque production. The proposed technique simplifies the SRM control in order to cut down the complexity and cost; it offers easy implementation and can be used for sensor and sensorless operation of SRM drives. It also provides an eligible candidate for industrial applications as the optimization strategy uses an analytical solution. For adequate modeling, the nonlinear magnetization characteristics of the SRM are obtained using finite element analysis. The SRM, converter, and control algorithm are modeled using the MATLAB/Simulink environment. The simulation results are compared with a closed-loop switch-on angle controller in order to show the feasibility of the proposed control technique. In addition, experimental results are obtained to prove the promising performance and simplicity of the proposed controller.

Key words: Switched reluctance motor, adaptive control, excitation angles, switch-on angle, switch-off angle, finite element analysis, MATLAB/Simulink

1. Introduction

The switched reluctance motor (SRM) is the simplest of all electric machines. It promises a reliable and low-cost variable-speed drive for several industrial applications [1–3]. However, the doubly salient structure causes highly nonlinear magnetic characteristics, which complicate the control of SRM drives [4, 5]. The SRM control strategy depends on inductance profile and requires an online adaptive control strategy to achieve high performance over a wide range of operating speeds [6–8].

In many applications, it is desirable to achieve the highest torque/ampere ratio over the widest range of possible speeds [9–11]. The developed torque of SRMs can be optimized by applying appropriate switch-

*Correspondence: m_hamouda26@mans.edu.eg

on (θ_{on}) and switch-off (θ_{off}) angles, but this may require sophisticated and complex digital controllers for real-time variation of switching angles as a function of motor current and speed [9, 12].

For decades, many types of research have been directed towards optimizing SRM performance based on the optimum solution for θ_{on} and θ_{off} angles. Using the ideal inductance profile, the conventional approach for θ_{on} was developed [12]. This solution can provide acceptable performance over a limited speed range [13]. In [5], the conventional approach was used to obtain an initial value of θ_{on}, and then within a certain range around this initial value an experiment was conducted to find the most efficient set of angles. In [6], a continuous tuning of θ_{on} under steady state was used to minimize total power consumption, but the control strategy depended on energizing switching angles and required a complicated process to shorten its searching time. In [4], a closed-loop θ_{on} control was designed to force the first peak of phase current to occur at the angle where rotor poles begin to overlap with stator poles (θ_m). This method requires two subalgorithms to monitor the first peak of phase current and its position. In [7], the excitation angles were optimized based on a fuzzy adaptive controller, which required good experimental knowledge of machine performance. In [13], an analytical solution was developed for excitation angle optimization. However, this method neglects stator resistance, which has a great effect on current profile. In [14], the field reconstruction method was used for switching angle optimization. It may deliver a fast but complicated solution. In [15], automatic control of switch-off angle in the face of switch-on angle automatic control was introduced to maximize drive efficiency. The formula of optimized switch-off angle as a function of speed and reference current magnitude was obtained from the experimental results.

In this paper, an adaptive control technique for optimum θ_{on} and θ_{off} angles is developed. The proposed technique uses an analytical solution that can provide an eligible candidate for industrial applications. It cuts down the complexity and provides a fast and accurate solution that offers simple structure, easy and low cost of implementation, and high dynamics. It can provide optimum motor performance over the possible range of operating speeds. It does not basically require experimental measurements; the inductance data can be obtained easily using finite element analysis (FEA).

The rest of this paper is organized as follows: Section 2 presents the problem description. Section 3 illustrates the proposed controller for optimum θ_{on} and θ_{off} angles. Section 4 and Section 5 contain the simulation and experimental results, respectively. Finally, Section 6 gives the conclusions drawn from this research.

2. Problem description

The SRM cannot run directly from a DC or AC line; it requires discrete commutation from one phase to another [16]. The control strategy of SRM drives mainly depends on its inherited inductance profile. For the sake of simplicity, a linear inductance profile is considered for explanation as shown in Figures 1a and 1b. The motor coils must be excited in the increasing inductance zone ($dL/d\theta > 0$), and they should be deenergized before the negative inductance zone ($dL/d\theta < 0$) in order to avoid negative torque production. The amount of allowed time for phase current to rise/fall is a function of motor speed, current magnitude, and θ_{on} and θ_{off} angles. The motor current profile differs greatly for low- and high-speed operation. At low speeds, the motor current can rise and decay quickly to reach its commanded reference value. Therefore, the switch-on instant can be delayed (close to θ_m) as illustrated in Figure 1a. On the contrary, at high speeds, the phase current can neither rise nor decay quickly enough to reach its preferred level. For that reason, the motor phase winding is switched on early to allow the phase current to reach its desired level, as shown in Figure 1b [3–5]. Therefore, the optimum θ_{on} should satisfy two conditions [4–6].

1. It should make the phase current reach its reference value.
2. It should force the first peak of phase current to occur at angle θ_m.

On the other hand, the optimum θ_{off} should make phase current decay to zero at θ_z. If the phase current decayed to zero after θ_z, a considerable amount of negative torque will be produced. In addition, if the current falls to zero before θ_z, the amount of generated positive torque will be decreased.

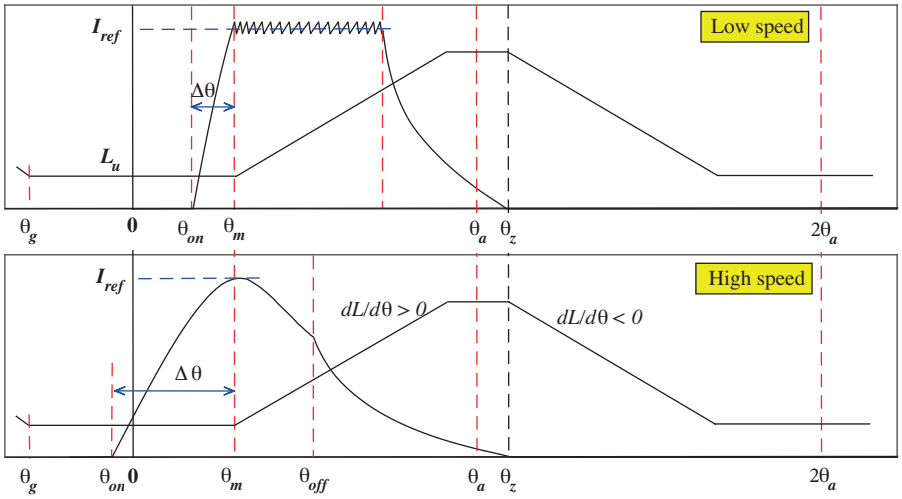

Figure 1. Ideal inductance and optimum current waveforms at a) low speed, b) high speed.

3. The proposed control technique

The motor for which the analysis is applied is a 6/4 three-phase SRM. Its magnetic circuit structure and main geometry configurations are shown in Figure 2. The motor dimensional and control parameters are given in the Table. As FEA is widely accepted for SRM characteristics calculation and performance analysis [17, 18], it is used to obtain the magnetization characteristics of the 6/4 SRM. Figure 3 shows the FEA-calculated inductance $L(i,\theta)$ and torque $T(i,\theta)$ characteristics. The unaligned and aligned positions are defined by angle $\theta = 0°$ and angle $\theta = 45°$, respectively.

Table 1. The design data of 6/4 SRM prototype in *mm*.

Parameter	**Value**	**Parameter**	**Value**
Output power	2.5 hp	Stator pole arc angle (β_s)	29°
Rated voltage	60 V	Rotor pole arc angle (β_r)	31°
Rated speed	1500 r/min	Air gap length (l_g)	0.4
Yoke outside diameter (D_{oy})	135	Stack length	90
Shaft diameter (D_{sh})	27	Unaligned inductance (L_u)	0.8 mH
Bore diameter (D_{bore})	74.2	Aligned inductance (L_a)	5 mH
Height of stator pole (h_{ts})	18	θ_m	12.5°
Height of rotor pole (h_{tr})	13	$\theta_a = \theta_z$	45°
Turns per phase	64	Core material	M-27 steel

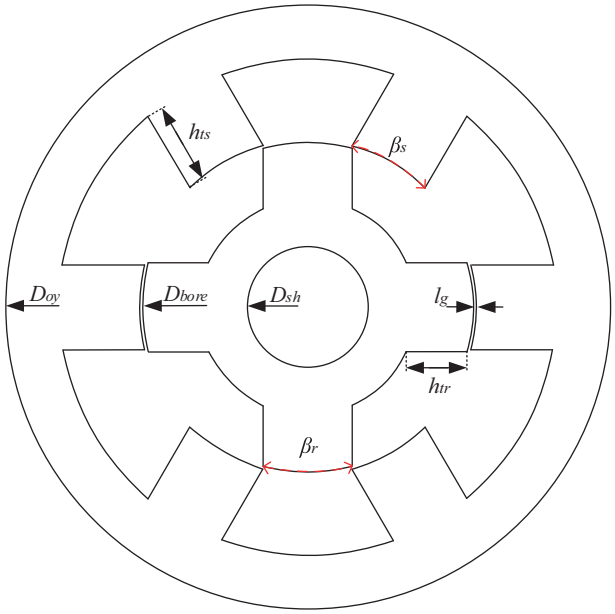

Figure 2. The basic geometrical dimensions of the SRM.

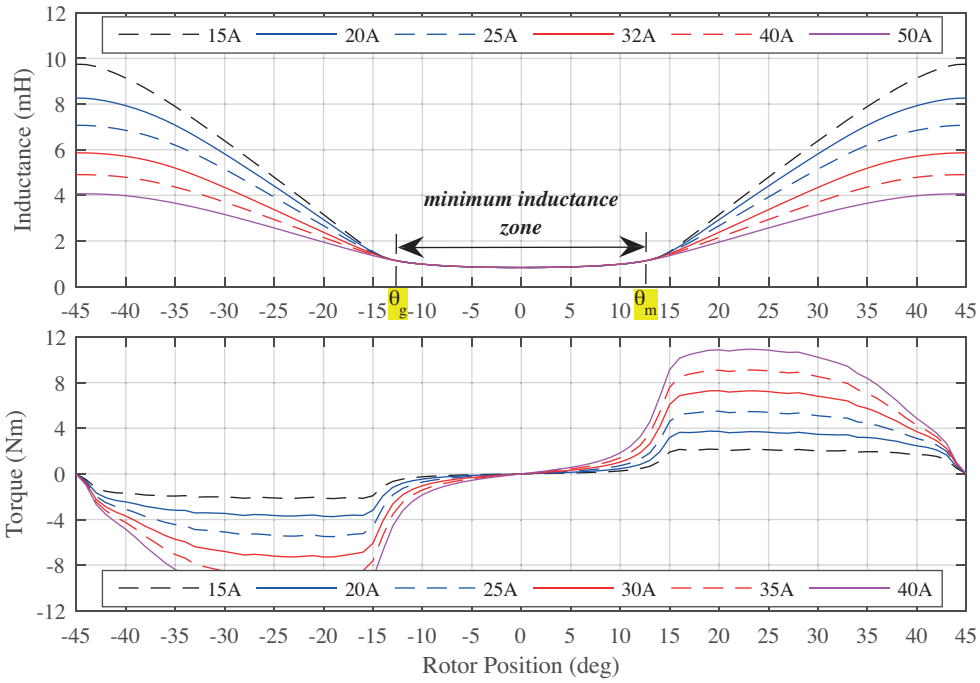

Figure 3. The FEA-calculated inductance $L(i,\theta)$ and static torque $T(i,\theta)$ characteristics.

3.1. Determination of optimum θ_{on}

The conventional approach for optimum θ_{on} is given as [5, 12]:

$$\theta_{on} = \theta_m - \frac{L_u I_{ref} \omega}{V_{dc}}, \tag{1}$$

where L_u is the minimum inductance, V_{dc} is the DC bus voltage, I_{ref} is the reference current, and ω is the rotor speed. Eq. (1) assumes that the phase-inductance is constant over region $[\theta_g,\ \theta_m]$. This approach can give reasonable performance under low speeds (up to base speed) unless θ_{on} becomes less than θ_g. For speed higher than rated speed, Eq. (1) starts to break down as back-emf voltage becomes more prominent.

The determination of optimum θ_{on} over a wide range of speed control depends on the accurate estimation of back-emf voltage. This can be achieved if the real inductance profile of the SRM is considered.

We start from the voltage equation, as follows [19, 20]:

$$V = Ri + L(i,\theta)\frac{di}{dt} + \frac{dL(i,\theta)}{d\theta}i\omega, \tag{2}$$

where V is the phase voltage and R is the phase resistance. Solving the voltage equation for phase current (i) during its energizing process gives:

$$i(t) = \frac{V_{dc}}{R + K_b\omega}[1 - e^{-(\frac{R + K_b\omega}{L_u})t_r}], \tag{3}$$

where $k_b = dL(i,\theta)/d\theta$. t_r is the required rise time for phase current to reach I_{ref}:

$$t_r = \frac{-L(i,\theta)}{R + K_b\omega} ln[1 - I_{ref}(\frac{R + K_b\omega}{V_{dc}})]. \tag{4}$$

In order to get the first peak of phase current at θ_m, θ_{on} should be advanced by ωt_r and θ_{on} becomes:

$$\theta_{on} = \theta_m - \omega t_r = \theta_m - \omega\frac{-L(i,\theta)}{R + K_b\omega} ln[1 - I_{ref}(\frac{R + K_b\omega}{V_{dc}})]. \tag{5}$$

Despite Eq. (5) giving the optimum solution of θ_{on}, it represents θ_{on} as a function of multiple variables (θ_m, ω, R, $L(i,\theta)$, k_b, I_{ref}, and V_{dc}). R and V_{dc} have almost constant values. θ_m is the angle at which rotor poles begin to overlap with stator poles. It depends on motor geometrical structure and is found to be 12.5°. ω and I_{ref} are control variables. Therefore, the determination of optimum θ_{on} depends mainly on $L(i,\theta)$ and its slope $k_b(i,\theta)$.

3.1.1. Accurate calculation of $L(i,\theta)$ and $k_b(i,\theta)$

The analysis of the inductance profile reveals the fact that in the minimum inductance zone $L(i,\theta)$ is only a function of rotor position $L(i,\theta) = L(\theta)$ (see Figure 3). Based on that fact, $L(i,\theta)$ can be fitted against θ using an exponential function as given by Eq. (6). After that, $k_b(i,\theta)$ can be calculated as the derivative of inductance as illustrated by Eq. (7). It should be noted that $k_b(i,\theta)$ is negative over $[\theta_g, 0]$ and positive over $[0, \theta_m]$.

$$L = ae^{b|\theta|} + c, \qquad \theta_g \le \theta \le \theta_m \tag{6}$$

$$k_b(i,\theta) = \begin{cases} -dL(i,\theta)/d\theta = -abe^{b|\theta|}, & (\theta_g \le \theta \le 0) \\ +dL(i,\theta)/d\theta = +abe^{b|\theta|}, & (0 \le \theta \le \theta_m) \end{cases} \tag{7}$$

Here, $a = 0.01161, b = 0.261$, and $c = 0.8173$ are fitting coefficients. The coefficients with 95% confidence bounds are calculated using the MATLAB fitting toolbox. Figure 4a shows a comparison between FEA-calculated inductance and its fitting curve. The variation of $k_b(i,\theta)$ against rotor position is given in Figure 4b.

The accurate fitting of $L(i,\theta)$ and $k_b(i,\theta)$ is not enough for accurate determination of optimum θ_{on}. According to Eq. (5), θ_{on} is calculated backward from θ_m. As given by Figure 1 but under consideration of the actual inductance profile, the difference between θ_m and θ_{on} is directly proportional to motor speed. As the motor speed increases, the difference ($\triangle\theta = \theta_m - \theta_{on}$) increases. Hence, for accurate determination of θ_{on}, the effective amount of inductance $L(i,\theta)$ and $k_b(i,\theta)$ should be calculated over interval $\triangle\theta$. In order to achieve that, an initial value for θ_{on} is required.

The calculation procedure for accurate θ_{on} is shown in Figure 5. First, an initial value for the switch-on angle is calculated using the conventional approach that is given by Eq. (1). Then the effective values of $L(i,\theta)$ and $k_b(i,\theta)$ are calculated as the average values over the period $[\theta_{on}, \theta_m]$ based on Eqs. (6) and (7). Finally, these values are used to determine the optimum θ_{on} accurately using equation (5).

It should be noted that the initial calculation of θ_{on} using the conventional approach may have a little impact on the effective values of $L(i,\theta)$ and $k_b(i,\theta)$. This impact can be eliminated by adding an additional stage that calculates effective values of $L(i,\theta)$ and $k_b(i,\theta)$ as a function of accurate θ_{on} if required. The effective values of $L(i,\theta)$ and $k_b(i,\theta)$ are plotted and fitted against initial θ_{on} as shown in Figures 6a and 6b respectively. For easy implementation, these effective values are fitted against initial θ_{on} as third-degree polynomials as follows:

$$L(i,\theta)_{eff} = a_1\theta_{on}^3 + a_2\theta_{on}^2 + a_3\theta_{on} + a_4, \tag{8}$$

$$k_b(i,\theta)_{eff} = b_1\theta_{on}^3 + b_2\theta_{on}^2 + b_3\theta_{on} + b_4, \tag{9}$$

where $a_1 = 1.718554e^{-08}, a_2 = 6.45122e^{-07}, a_3 = 5.725676e^{-06}, a_4 = 9.0429e^{-04}$ and $b_1 = 8.8571e^{-09}, b_2 = 1.0006e^{-07}, b_3 = 1.7266e^{-06}, b_4 = 2.2657e^{-05}$ are fitting coefficients that are calculated using the MATLAB fitting toolbox.

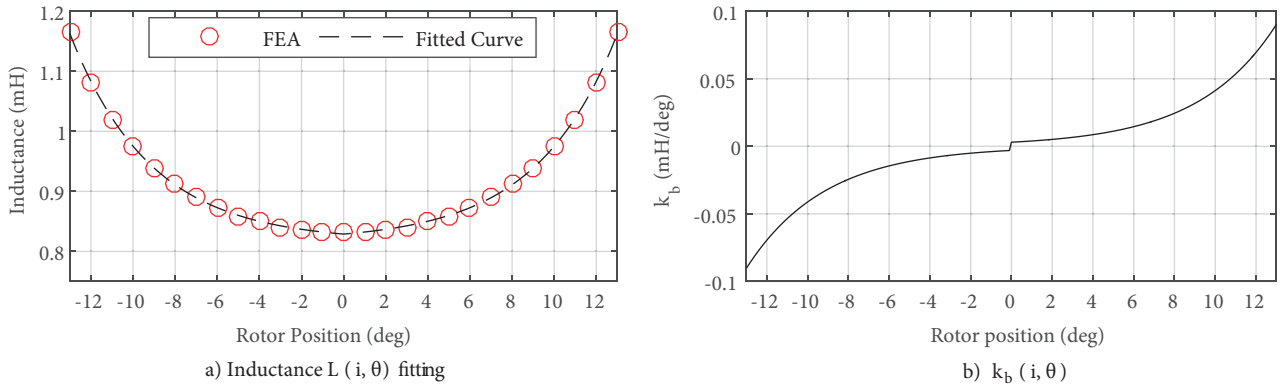

Figure 4. Fitting curve for $L(i,\theta)$ and $k_b(i,\theta)$ in minimum inductance zone.

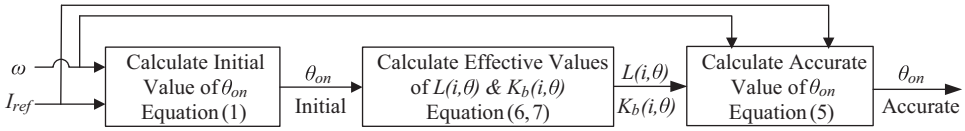

Figure 5. The procedure for accurate calculation of optimum θ_{on}.

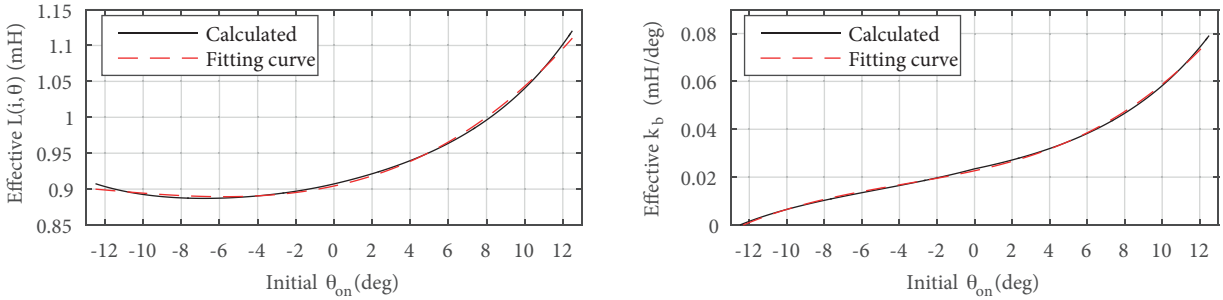

a) The effective value of L (i, θ). b) The effective value of k_b (i, θ).

Figure 6. Fitting for the effective values of $L(i,\theta)$ and $k_b(i,\theta)$.

3.2. Determination of optimum θ_{off}

As mentioned earlier, the optimum θ_{off} should make motor phase current decay to zero at θ_z. The analytical solution for θ_{off} is very complicated because inductance at the instant of switch-off is a function of current magnitude and rotor position. A simplified solution can be introduced based on the fact that the flux rise time is equal to its falling time under single pulse control with neglected stator resistance [13]. Figure 7 shows the phase flux linkage and phase current in an electric period. After the phase winding is switched on, the phase flux-linkage rises up from zero, reaching its peak at θ_{off}. Meanwhile, after the phase winding is switched off, the flux-linkage falls down, reaching zero at θ_z. With the flux-linkage's rising time (t_{rise}) and falling time (t_{fall}):

$$t_{rise} = \frac{\theta_{off} - \theta_{on}}{\omega} = t_{fall} = \frac{\theta_z - \theta_{off}}{\omega} \quad \Rightarrow \quad \theta_{off} = \frac{1}{2}(\theta_{on} + \theta_z). \tag{10}$$

Eq. (10) is derived based on single pulse control under high-speed operation. This equation starts to introduce a noticeable error while the speed is decreasing. The error becomes unacceptable under current chopping mode. This error can be handled with a compensation factor k, and Eq. (10) becomes:

$$\theta_{off} = \frac{1}{2}(\theta_{on} + \theta_z) + k(1 + w\frac{I_{max}}{I_{ref}}), \tag{11}$$

where k is a curve-fitting parameter that is adjusted with motor speed as a third-degree polynomial as given in Figure 8. I_{max} is the maximum permissible current that can follow in motor winding. Mostly, $I_{ref} = I_{max}$ during the chopping process. $w = 0.02$ is a weight factor to suitably adjust the increase of θ_{off} compensation in the case of $I_{ref} < I_{max}$. In general, in order to avoid production of negative torque, angle θ_z should be equal to θ_a. This may differ slightly according to the motor's inherited inductance profile. In this paper, θ_z is set to 45°. The structure of the θ_{off} controller is illustrated in Figure 9.

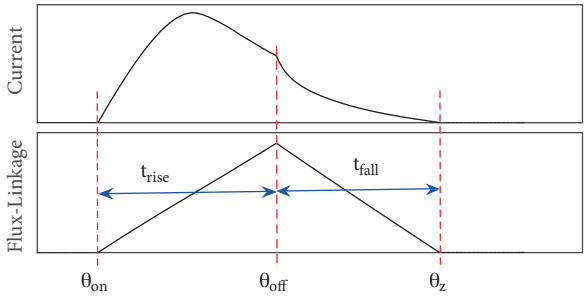

Figure 7. Flux-linkage against phase current.

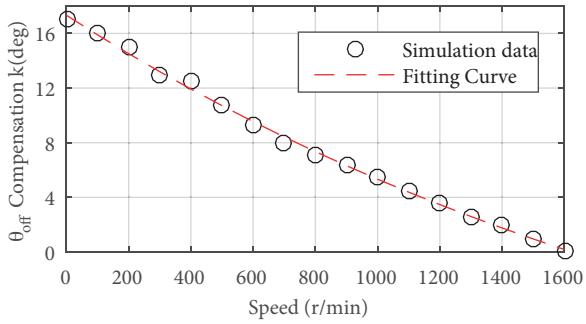

Figure 8. Switch-off angle compensation (k).

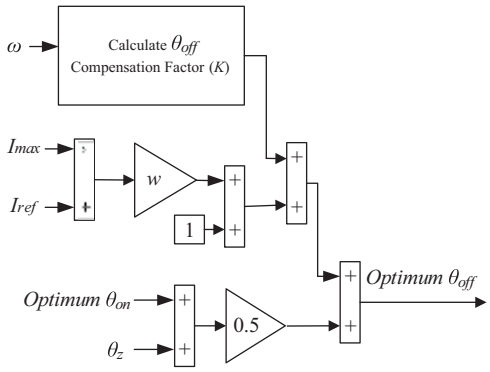

Figure 9. The structure of θ_{off} controller.

4. Simulation results and discussion

For clear verification of the proposed control technique, a closed-loop switch-on angle (CL θ_{on}) is used for the purpose of comparison [4]. Despite the other types of θ_{on} control techniques, CL θ_{on} is the best to guarantee an optimum solution for θ_{on} as it is a closed loop control. This controller forces the first peak of phase current (θ_{peak}) to occur at θ_m and also allows the peak phase current to reach its reference level. The structure of the CL θ_{on} controller is shown in Figure 10. It compares the peak value of phase current (I_{peak}) to its reference level (I_{ref}), and the angle of the first peak position (θ_{peak}) to θ_m. The error signal is processed through a PID controller whose output compensates the conventional approach. The controller parameters are $KP\theta = 0.5$ and $KPI = 0.2°/A$, and PID gains are $KP = 0.5, KI = 12,$ and $KD = -0.004$.

A complete simulation model of the 6/4 SRM, its drive system, and the control algorithms is achieved using the MATLAB/Simulink environment. The FEA-calculated magnetization characteristics are used for SRM simulation in the form of lookup tables [21, 22].

The motor performance under a sudden change in speed and load torque is shown in Figures 11a– 11d. The motor starts with a constant load torque of 4.5 Nm and then load torque is decreased from 4.5 Nm to 3 Nm at 0.7 s. The speed is suddenly changed from 1500 r/min to 2500 r/min at 0.9 s as shown in Figure 11a. The online automatic control of θ_{on} is shown in Figure 11b. θ_{on} of the proposed controller has a clear difference from the CL θ_{on} controller because of the required settling time for the CL θ_{on} controller to reach steady state. The proposed controller provides the optimum solution of θ_{on} instantaneously according to motor speed and current magnitude. Its performance depends on the effective values of $L(i,\theta)$ and $k_b(i,\theta)$. The proposed control

technique provides an adaptive solution for θ_{on} by accurate determination of the effective values of $L(i,\theta)$ and $k_b(i,\theta)$ as illustrated in Figure 11c. It is clear that $L(i,\theta)$ and $k_b(i,\theta)$ are fully adaptive with motor speed and load torque. The online control of θ_{off} is given in Figure 11d.

A clear verification of optimum solution for θ_{on} and θ_{off} angles is given in Figures 11e– 11h. The proposed controller provides optimum θ_{on}, which forces the first peak of phase current to always occur at angle $\theta_m = 12.5^\circ$ (see Figure 11e). It also allows the peak value of phase current (I_{peak}) to reach its recommended reference level as shown in Figures 11f and 11g. For the CL θ_{on} controller, despite it reaching a steady-state value of 12.5°, it needs settling time and provides lower dynamic performance compared to the proposed controller.

The production of no negative torque can be guaranteed as illustrated in Figure 11h. After the instant of switching off, the phase current decays to zero at angle $\theta_z \cong 45^\circ$, which ensures no production of negative torques. Thus, the switch-off angle is optimum over the entire speed range. The current, inductance, and torque waveforms at low and high speeds are shown in Figures 12a and 12b, respectively. It is clear that the position of the first peak of phase current occurs at the end of the minimum inductance zone ($\theta_m = 12.5^\circ$), the current decays to zero at $\theta_z \cong 45^\circ$, and the torque profile has no negative torque at all. This ensures the optimum solution of θ_{on} and θ_{off}.

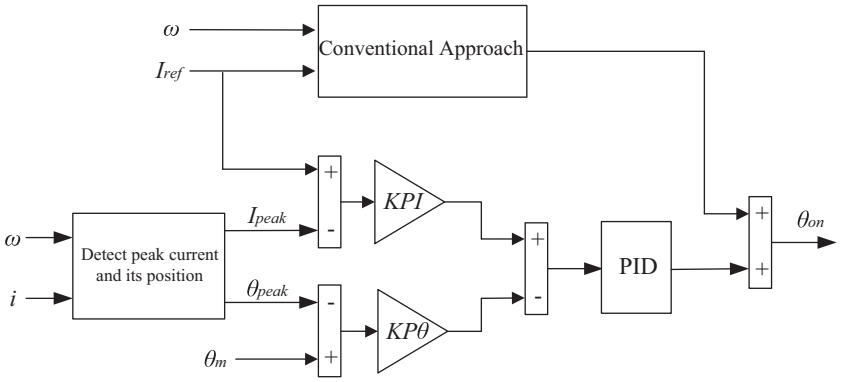

Figure 10. The structure of closed-loop switch-on angle controller (CL θ_{on} controller).

5. Experimental verification

The controller performance is experimentally verified with a 6/4 three-phase SRM. The SRM specifications are given in the Table. The control algorithm is implemented using a Texas Instruments TMS320F28379D digital signal processor (DSP). The SRM is coupled to an electromagnetic brake (MAGTORL model 4605c), which acts as a mechanical load. An absolute shaft encoder (RM44SI0010B10F2E10) is used to provide the absolute rotor position through a synchronous serial interface (SSI) that is connected to SPI terminals of the DSP through an interface circuit. The estimated variables (θ_{on}, θ_{off}, and phase rotor position) are output using the digital analog converters (DACs) of the DSP board. High-accuracy and linear LAH50-P current transducers (CTs) are used for phase current measurements. The phase voltages and supply voltage are measured using a high-speed and linearity-based op-amp circuit. A three-phase transformer, three-phase diode rectifier, and capacitor are used to provide DC power. The data are collected and plotted using a data acquisition board (DAQ NI USB-6009) and LabView software. The DSP is programmed using MATLAB/Simulink with the C2000 microcontroller support package in addition to Code Composer Studio (CCS) software. Figure 13 illustrates

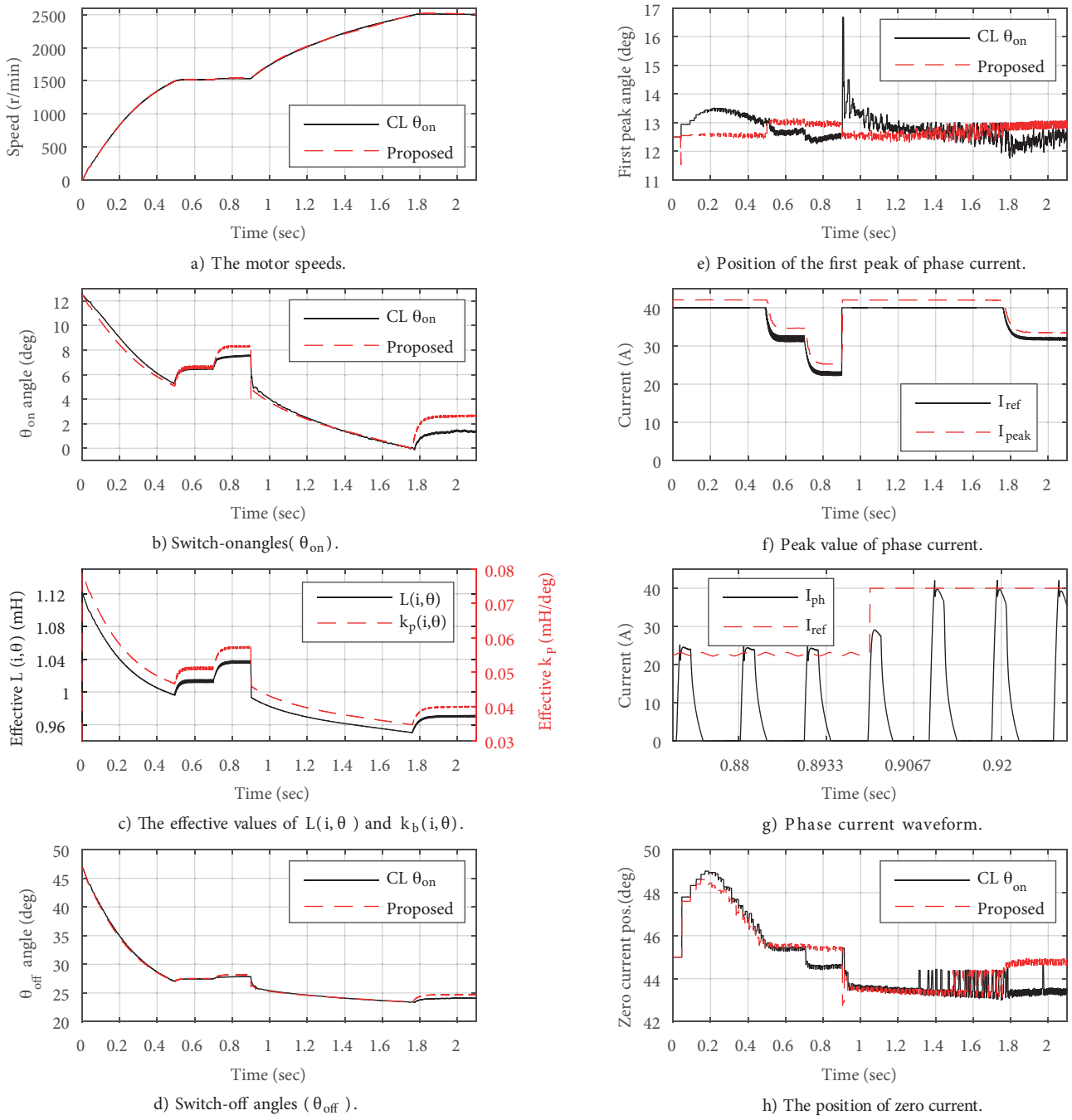

Figure 11. The simulation results under sudden change in speed and load torque.

the schematic diagram of the measurement platform while Figure 14 shows the practical implementation of this platform.

Figures 15a– 15f show the controller behavior under transient conditions. They illustrate the actual motor speed and θ_{on} and θ_{off} variation under a sudden step change in speed from 200 r/min to 1600 r/min. Both the original and filtered signals are included. A clear adjustment of θ_{on} and θ_{off} is seen to track changes

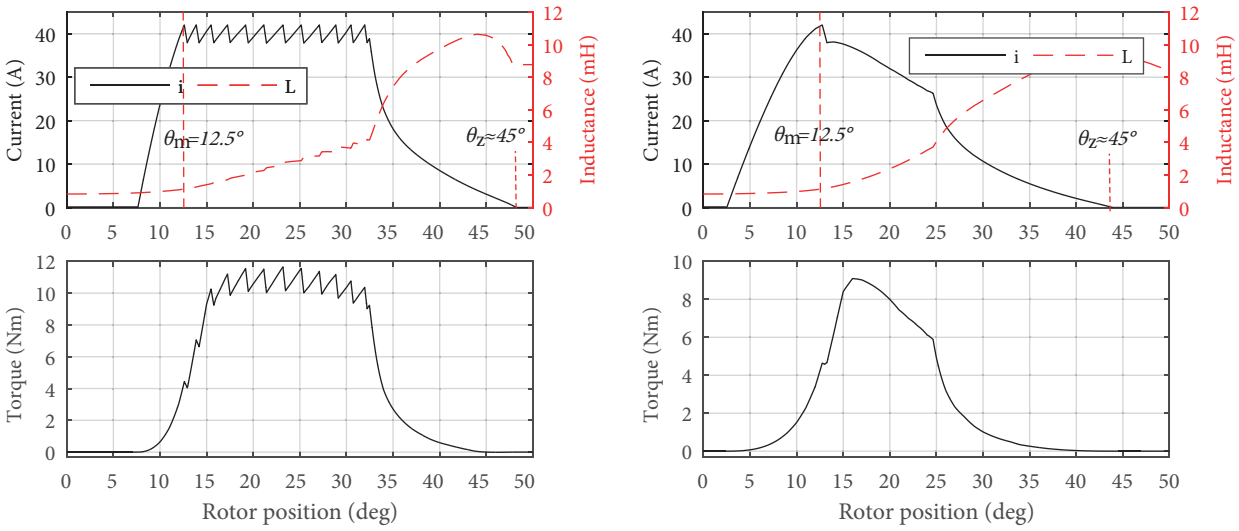

a) At low speed of 1000 r/ min.

b) At high speed of 2000 r/ min.

Figure 12. The current, inductance, and torque wave-forms.

in motor speed and current magnitude. As the motor speeds up, θ_{on} decreases automatically to allow motor current to reach its reference level. θ_{off} is also adjusted to force current decay to zero at θ_z.

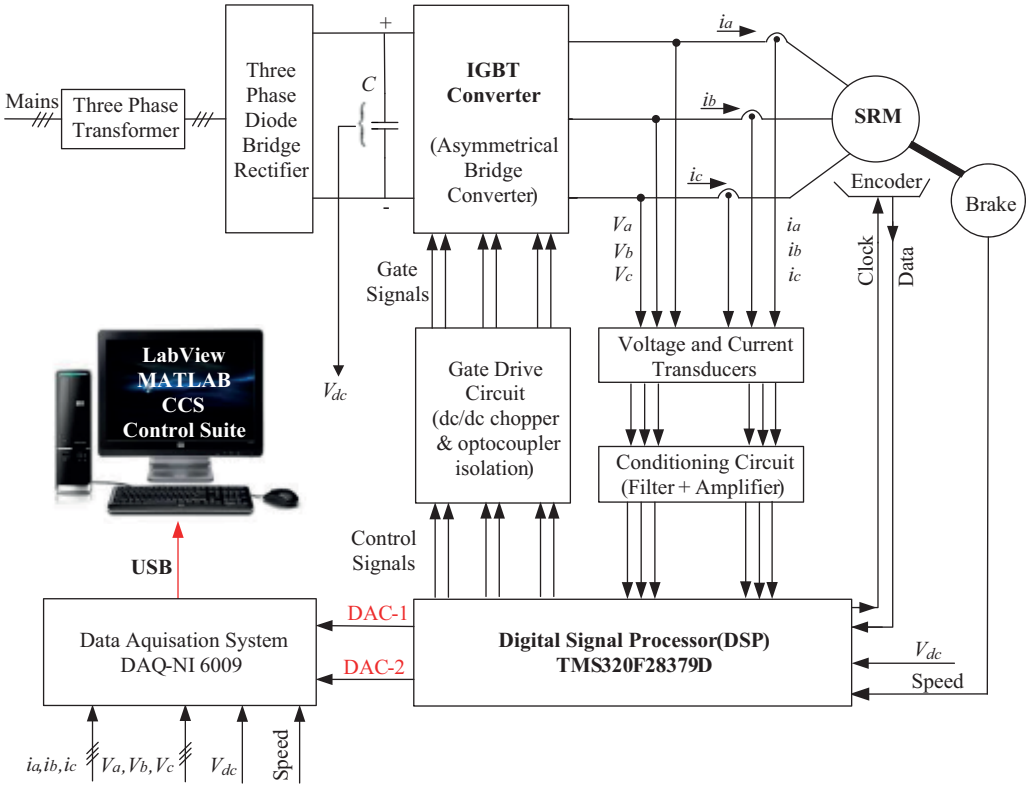

Figure 13. Schematic diagram of the measurement platform.

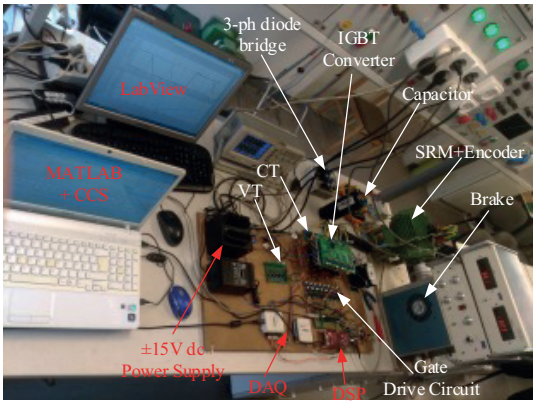

Figure 14. Practical implementation of the measurement platform.

A detailed verification of the performance and effectiveness of the proposed control technique is given in Figures 16a– 16f. This figure gives the experimental phase current against rotor position at a variety of operating speeds (704 r/min, 1071 r/min, 1317 r/min, 1514 r/min, 1846 r/min, 1966 r/min). At all the operating speeds,

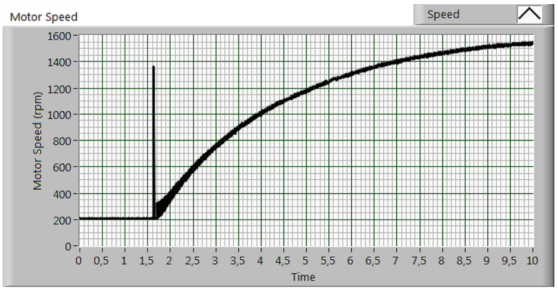

a) The motor speed

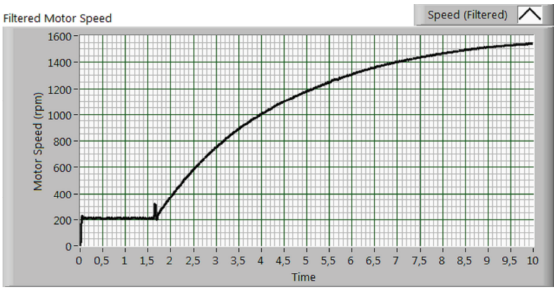

d) The filtered motor speed

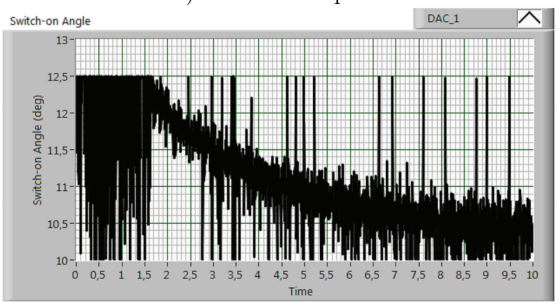

b) variation of θ_{on}

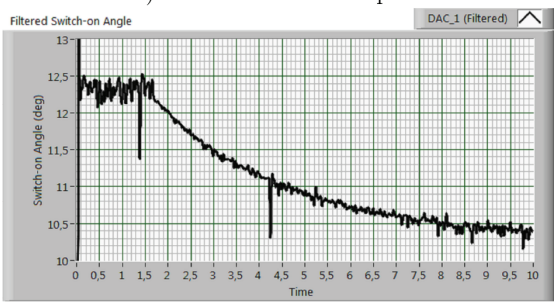

e) The filtered variation of θ_{on}

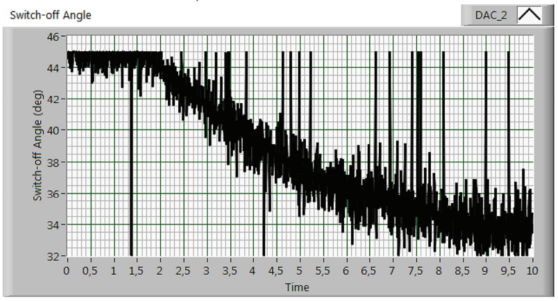

c) variation of θ_{off}

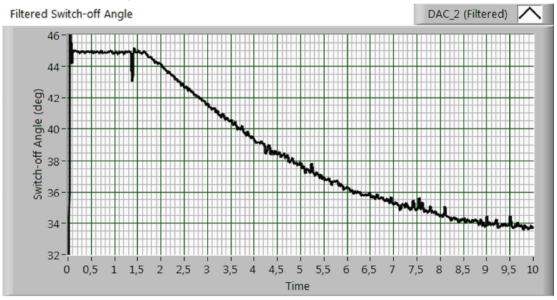

f) The filtered variation of θ_{off}

Figure 15. Experimental results under sudden step change in speed.

the controller provides a very good adjustment of θ_{on} to force the first peak of phase current to always occur at $\theta_m = 12.5°$. It also controls θ_{off} to make phase current decay to zero at $\theta_z \cong 45°$.

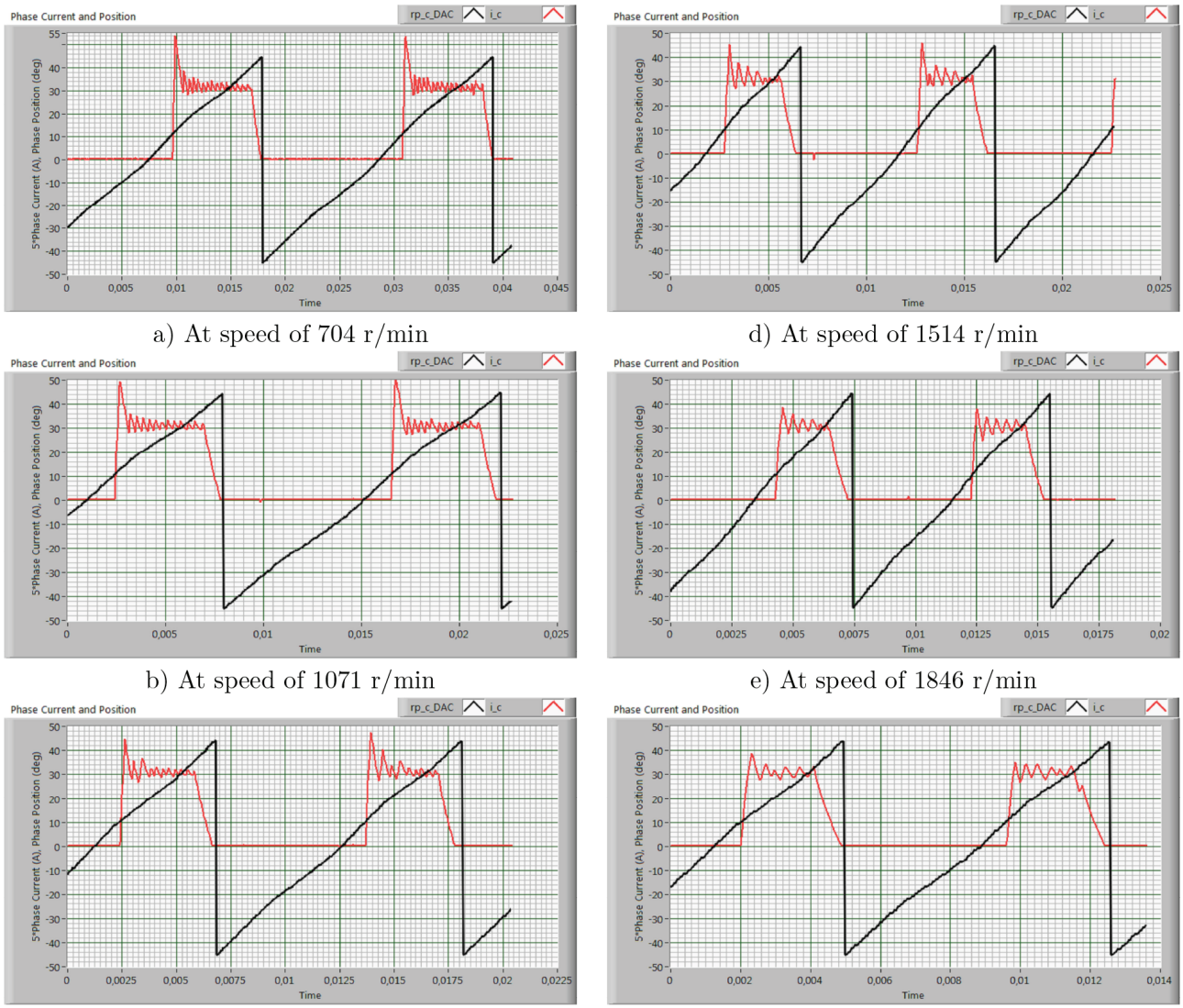

a) At speed of 704 r/min

d) At speed of 1514 r/min

b) At speed of 1071 r/min

e) At speed of 1846 r/min

c) At speed of 1317 r/min

f) At speed of 1966 r/min

Figure 16. Experimental results at variety of operating speeds.

6. Conclusions

This paper presented an adaptive analytical solution for optimum θ_{on} and θ_{off} angles of SRM drives over a wide range of speed control. The proposed control technique determines the optimum θ_{on} that provides the most efficient operation. It accurately considers the effect of back-emf voltage by adaptive calculation of the effective amount of phase inductance $L(i,\theta)$ and its derivative $k_b(i,\theta)$. In addition, it calculates the optimum θ_{off} in order to avoid production of negative torque even at high speeds. The proposed control technique uses analytical solutions that offer a simple structure, low cost of implementation, and high dynamics. The motor,

its converter, and control algorithms are modeled using MATLAB/Simulink. The experimental and simulation results show that the proposed technique provides optimum operation over an extended speed range.

References

[1] Chen H, Yang Z, Cheng H. Average torque control of switched reluctance machine drives for electric vehicles. IEEE T Power Electr 2015; 9: 459-468.

[2] Hamouda M, Amin ARA, Gouda E. Experimental investigation of switched reluctance motor detailed performance under balanced and unbalanced operation. Mansoura Engineering Journal 2015; 40: 29-40.

[3] Wang X, Yang Z, Wang T, He D, Huo Y, Cheng H, Yu G. Design of a wide speed range control strategy of switched reluctance motor for electric vehicles. In: IEEE 2015 International Conference on Information and Automation; 8–10 August 2015; Lijiang, China. New York, NY, USA: IEEE. pp. 294-299.

[4] Sozer Y, Torrey DA, Mese E. Automatic control of excitation parameters for switched-reluctance motor drives. IEEE T Power Electr 2003; 18: 594-603.

[5] Morón C, Tremps E, Ramirez P, Garcia A, Somolinos JA. Performance optimization in switched reluctance motor drives with online commutation angle control. IEEE T Energy Conver 2003; 18: 448-457.

[6] Shun-Chung W, Wen-Han L. Turn-on angle searching strategy for optimized efficiency drive of switched reluctance motors. In: 30th Annual Conference of Industrial Electronics Society; 2–6 November 2004; Busan, South Korea. New York, NY, USA: IEEE. pp. 1873-1878.

[7] Moradi Cheshmehbeigi H, Yari S, Yari AR, Afjei E. Self-tuning approach to optimization of excitation angles for switched reluctance motor drives using fuzzy adaptive controller. In: 13th European Conference on Power Electronics and Applications; 8–10 September 2009; Barcelona, Spain. New York, NY, USA: IEEE. pp. 1-10.

[8] Shahabi A, Rashidi A, Afshoon M, Saghaian Nejad SM. Commutation angles adjustment in SRM drives to reduce torque ripple below the motor base speed. Turk J Electr Eng Co 2016; 24: 669-682.

[9] Argeseanu A, Ritchie E, Leban K. Torque optimization algorithm for SRM drives using a robust predictive strategy. In: 12th International Conference on Optimization of Electrical and Electronic Equipment; 20–22 May 2010; Brasov, Romania. New York, NY, USA: IEEE. pp. 252-257.

[10] Orthmann R, Schoner HP. Turn-off angle control of switched reluctance motors for optimum torque output. In: 5th European conference on power electronics and applications; 13–16 September 1993; Brighton, UK. New York, NY, USA: IEEE. pp. 20-25.

[11] Jian LZ, Nguyen LMT, Nguyen LT, Phan XL. Switching-off angle control for switched reluctance motor using adaptive neural fuzzy inference system. International Journal of Energy and Power Engineering 2015; 4: 39-45

[12] Miller TJE, Bicknell WH, Szczesny PM. Microcomputer control of switched reluctance motor. IEEE T Ind Appl 1986; IA-22: 708-715.

[13] Xu YZ, Zhong R, Chen L, Lu SL. Analytical method to optimise turn-on angle and turn-off angle for switched reluctance motor drives. IET Electr Power App 2012; 6: 593-603.

[14] Lin C, Fahimi B. Optimization of commutation angles in SRM drives using FRM. In: IEEE 2012 Transportation Electrification Conference and Expo; 18–20 June 2012; Dearborn, MI, USA. New York, NY, USA: IEEE. pp. 1-6.

[15] Sozer Y, Torrey DA. Optimal turn-off angle control in the face of automatic turn-on angle control for switched-reluctance motors. IET Electr Power App 2007; 1: 395-401.

[16] Hamouda M, Amin ARA, Gouda E. A drive system design and implementation for switched reluctance motor based on wide range speed control. In: 17th International Middle East Power System Conference; 15–17 December 2015, Mansoura, Egypt. New York, NY, USA: IEEE. pp. 1-8.

[17] Kiyota K, Kakishima T, Sugimoto H, Chiba A. Comparison of the test result and 3D-FEM analysis at the knee point of a 60 kW SRM for a HEV. IEEE T Magn 2013; 49: 2291-2294.

[18] Song S, Ge L, Ma S, Zhang M, Wang L. Accurate measurement and detailed evaluation of static electromagnetic characteristics of switched reluctance machines. IEEE T Instrum Meas 2015; 64: 704-714

[19] Krishnan R. Switched Reluctance Motor Drives: Modeling, Simulation, Analysis, Design, and Applications. Boca Raton, FL, USA: CRC Press, 2001.

[20] Rodrigues M, Branco PJC, Suemitsu W. Fuzzy logic torque ripple reduction by turn-off angle compensation for switched reluctance motors. IEEE T Ind Electron 2001; 43: 711-715.

[21] Husain I, Hossain SA. Modeling, simulation, and control of switched reluctance motor drives. IEEE T Ind Electron 2005; 52: 1625-1634.

[22] Hamouda M, Szamel L. Accurate measurement and verification of static magnetization characteristics for switched reluctance motors. In: 19th International Middle East Power System Conference; 19–21 December 2017; Cairo, Egypt. New York, NY, USA: IEEE. pp. 993-998.